ELSEVIER

Biophysical Chemistry 53 (1994) 115–122

Biophysical Chemistry

Direct shape determination of ribosomal proteins in solution and within the ribosome by means of neutron scattering

Petra Nowotny [a,1], Martin Rühl [a], Volker Nowotny [a,1], Roland P. May [b], Nils Burkhardt [a], Helga Voss [a], Knud H. Nierhaus *,[a]

[a] *Max-Planck-Institut für Molekulare Genetik, Abteilung Wittmann, Ihnestrasse 73, D-14195 Berlin, Germany*
[b] *Institut Laue-Langevin, B.P. 156, F-38042 Grenoble Cedex 09, France*

Received 1 December 1993; accepted in revised form 25 January 1994

Abstract

Following the 'strategy of the glassy ribosome' single protonated ribosomal proteins (r-proteins) were reconstituted into deuterated 50S subunits of *Escherichia coli*. The deuteration of both rRNA and r-proteins were individually adjusted to such a degree that the ribosomal matrix appeared nearly homogeneous with respect to coherent neutron scattering and had a scattering density equivalent to a D_2O solution of about 90%. Neutron scattering of ribosomal subunits was recorded in reconstitution buffer containing three different concentrations of D_2O around 90% D_2O (contrast variation). The signal-to-noise ratio achieved allowed us to make a direct determination of the radii of gyration of r-proteins within the 50S subunit and thus provides the first information relating to the shape of these proteins in situ. We present the radii of gyration of 11 r-proteins incorporated into 50S subunits and of 9 isolated r-proteins in solution. In addition, the data concerning the overall dimensions of the r-proteins we report on indicate that conformational changes of at least two individual r-proteins occur during the assembly process of the ribosome.

Keywords: Neutron scattering; Ribosomal structure; Ribosomal proteins; Ribosomal assembly; Reconstitution of ribosomes; Guinier approximation

1. Introduction

A prerequisite for understanding protein biosynthesis is knowledge about the structure of ribosomes in sufficient detail. The ribosomal structure is highly complicated; in the case of the eubacterium *Escherichia coli* the ribosome consists of 54 different ribosomal proteins (r-proteins) and 3 rRNAs [1]. The most powerful technique, which might ultimately yield the structure at atomic resolution, is X-ray crystallography. Although remarkable progress has been made concerning the quality of ribosomal crystals [2], a crystallographic structure is not expected to be available for several more years.

For this reason it remains important to apply other methods to obtain information about the structure of the ribosome and its components at medium resolution, i.e. the shapes and positions in space of the

* Corresponding author.
[1] Present address: Washington University, School of Medicine, Center for Genetics in Medicine, Box 8232, 4566 Scott Avenue, St. Louis, MO 63110, USA.

SSDI 0301-4622(94)00082-U

r-proteins and rRNAs. The overall shape of the *E. coli* ribosome has been analyzed by electron microscopy (EM) and image reconstruction techniques [3] as well as by X-ray [4,5] and neutron small-angle scattering [6]. The arrangement of the ribosomal components, especially the distribution of epitopes of r-proteins on the surface of both subunits, has been investigated by immune electron microscopy and cross-linking [7–9]. The spatial distribution of r-proteins has been determined by neutron scattering [10,11].

The structure of isolated r-proteins could be solved to atomic resolution for L30, S5 and L12CTF [12–14] by X-ray crystallography. In addition hydrodynamic methods as well as different scattering techniques were extensively used, yielding the overall shape of a number of isolated r-proteins in solution (for a review, see Ref. [15]). However, neutron scattering is the only method available to date for analyzing the shape of r-proteins within the ribosomal complex. Radii of gyration (R_G, shape information) of the r-proteins of the 30S subunit were determined by Capel et al. [11], but unfortunately the reported R_G values suffered from high errors, up to $\pm 100\%$. Two reasons are mainly responsible for this high error level: (1) The R_G values were calculated as ancillary parameters in the determination of interprotein distances and could not be obtained with high precision for mathematical reasons; (2) the samples contained two deuterated r-proteins in a protonated ribosomal matrix, which results in an unfavorable signal-to-noise ratio because of the high incoherent background scattering of the matching buffer (for discussion, Ref. [10]). Recently, Harrison, May and Moore [16] obtained a more precise value of 23.5 ± 10 Å for the radius of gyration of protein S4 of the small ribosomal subunit by applying the three-isotope method (TIM) of Pavlov and Serdyuk [17]. TIM which, in principle, suppresses all scattering contributions except those from a selected component within a complex molecule requires, however, the preparation of three differently deuterated particles for every component to be studied.

Applying the 'strategy of the glassy ribosome' [18] we prepared samples containing a single protonated r-protein in an otherwise deuterated ribosomal matrix with different deuteration levels for ribosomal proteins and rRNA (see Section 2). Because the scattering densities of r-proteins and rRNAs were matched at a high deuteration level the reconstituted ribosomal matrix appeared to be almost homogeneous for neutrons in a solution containing about 90% D_2O. Thereby the coherent signal-to-noise ratio was improved significantly, and the radius of gyration of a protonated r-protein could be determined from a single scattering experiment. Here we present the radii of gyration of 11 r-proteins within the 50S subunit and of 9 isolated r-proteins in solution.

2. Materials and methods

2.1. Isolation of protonated components

The fermentation of *E. coli* cells (strain AB301, D10; $RNase^-$, met^-) in protonated medium and the isolation of ribosomal subunits followed Ref. [19]. The isolation of single protonated r-proteins from 50S subunits was carried out in a two step procedure: (1) Defined families of r-proteins were washed off the 50S subunits by increasing LiCl-concentrations; (2) subsequent application of HPLC techniques, either ion-exchange or reversed-phase chromatography, purified most of the r-proteins to homogeneity (for details, Refs. [20–22]).

2.2. Isolation of deuterated components

Fermentation of *E. coli* cells (MRE600) in deuterated medium as well as the isolation of deuterated rRNA and deuterated TP50 (fraction of total proteins of the 50S subunit) were described previously [22]. Elimination of single proteins was carried out by subjecting deuterated protein fractions to the HPLC isolation protocols described for protonated components and pooling all fractions not containing the protein to be excluded. If necessary the remaining protein fractions were purified further. The good maintenance of biological activity and the nearly quantitative recovery reached with HPLC methods [22] simplifies this step greatly and allows stoichiometric protein ratios to be retained in the recombined protein fractions.

2.3. Preparation of reconstituted particles

The preparation of the particles followed the 'strategy of the glassy ribosome' [18]. Deuterated

rRNA, isolated from cells grown in 76% D_2O, and deuterated TP50 derived from cells grown in 84% D_2O, together with a tenfold excess of one protonated r-protein were reconstituted and purified via zonal centrifugation; the activities of the resulting particles were confirmed by poly(U)-dependent poly(Phe) synthesis and the r-protein content was analyzed by two-dimensional gel electrophoresis (for further details, see Ref. [22]). In some cases (see Table 1) one protein was removed from the deuterated TP50 by means of HPLC techniques (see above). The corresponding protonated protein was added in stoichiometrical amount, and reconstitution was performed as reported elsewhere (for details and discussion, Ref. [10]).

2.4. Collection of neutron scattering data

The neutron scattering data were collected with the small-angle scattering facility D11 [23] at the Institut Laue-Langevin (ILL, Grenoble, France) as reported previously in detail [10]. Ribosome concentrations were of the order of 200 A_{260} units/ml (about 12.5 mg/ml), those of the isolated proteins of about 1 mg/ml and lower.

3. Results

Two sets of neutron scattering measurements were performed. The isolated proteins (H-Lx) were measured in a D_2O buffer to maximize the contrast and to minimize the incoherent scatter. After subtraction of electronic noise and buffer contributions the scattering curves were analyzed by the Guinier formalism. For proteins integrated into ribosomes (50S(Lx)), a more complex measurement had to be applied. We collected data for a Q range large enough to obtain sufficiently precise data for the ribosomal matrix. A correction for the presence of the ribosome was made possible by applying the contrast variation method.

For each sample, including a reference particle (a reconstituted 50S subunit containing no protonated r-protein), the scattering intensities were recorded at three different contrasts (nominally 99%, 95% and 90% D_2O). The data were corrected and scaled according to Ref. [10]. The scattering curves (shown for protein L3 as an example in Fig. 1a) were used to calculate the characteristic functions [24]. One of these is the contrast-independent I_s intensity profile where the zero-angle scattering from the reference particle is minimal. The reference-particle I_s profile does not vanish completely, but it decays very rapidly, much faster than the curves of particles containing labeled proteins (Fig. 1b). We suspect that the presence of zero-angle scattering can only be due either to the fact that the reconstituted particles exist as a multitude of nearly identical particles with a narrow distribution of differently deuterated components (protein and RNA)–i.e. to a isotopic population heterogeneity–or to unknown particles, e.g. from the dialysis bag, accumulated during the sample preparation. We could not find any proof for the

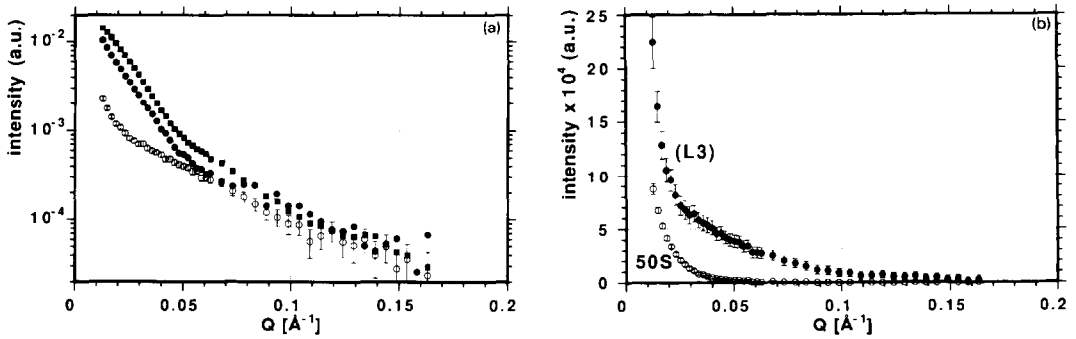

Fig. 1. (a) Contrast variation: Neutron scattering intensities of a 'glassy' (selectively deuterated; see text) ribosomal 50S subunit (*E. coli*) with protonated protein L3 at three different contrasts, nominally 90% (●), 95% (○) and 99% (■) ^2H_2O in the buffer solution. (b) Comparison of the scaled neutron scattering intensities of glassy 50S particles containing protonated protein L3 and of the reference particle (protein L3 deuterated like all other proteins of the subunit), calculated at the match point.

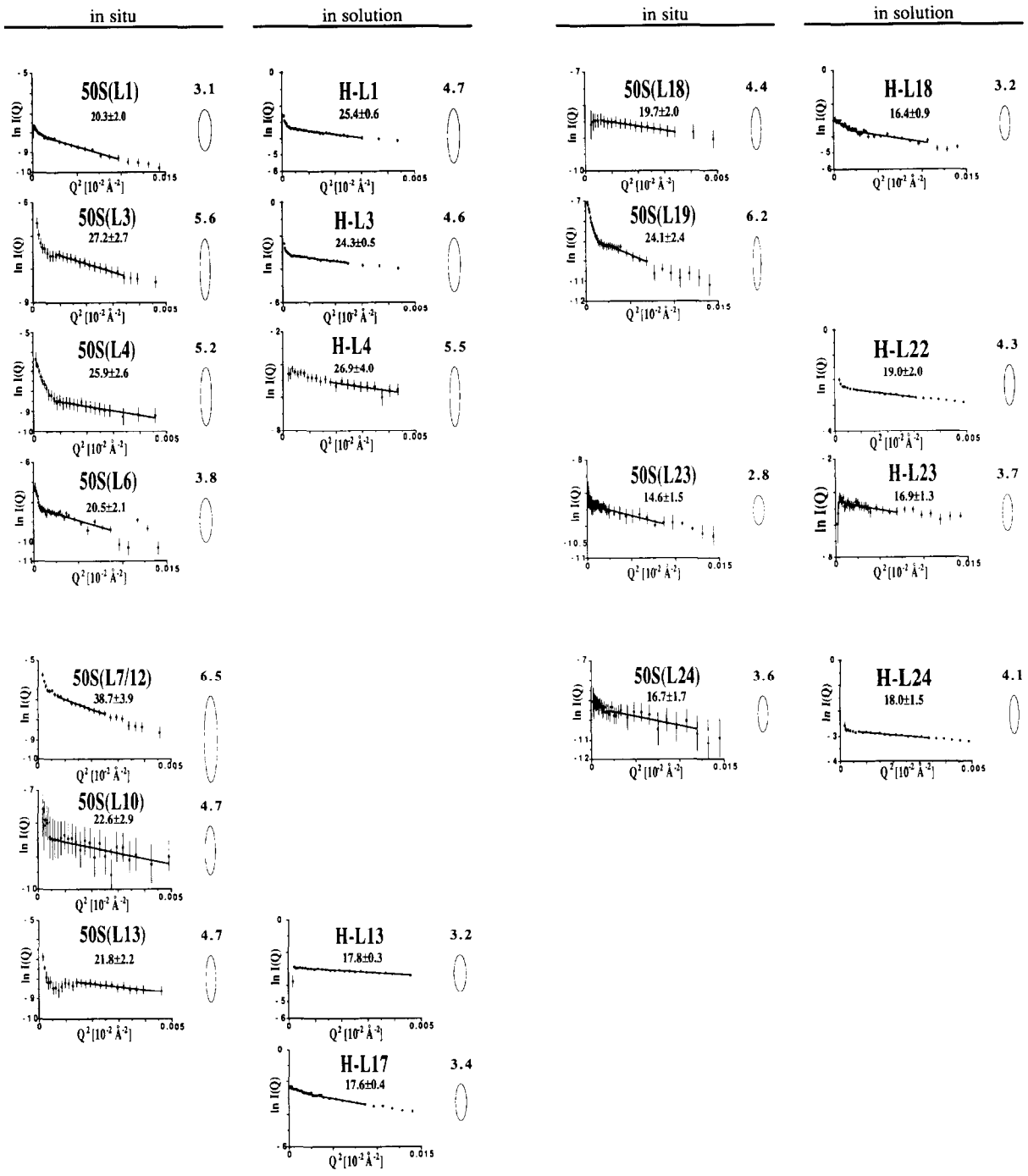

Fig. 2. Neutron scattering data of ribosomal proteins within the 50S subunit and isolated in solution: Guinier plots (columns 1 and 3), and the prolate ellipsoid of revolution equivalents (columns 2 and 4). 50S(Lx) and H-Lx mean the ribosomal protein Lx within the 50S subunit and isolated in solution, respectively; the corresponding radii of gyration are given within the Guinier plots in Å. The axial ratios of the ellipsoid equivalents are given above the ellipsoid symbols, the volume of an ellipsoid is proportional to the relative molecular mass of the respective protein.

second assumption. The absolute intensity of the zero-contrast scattering for the reference particle varied from one preparation to the next, but not its shape. We subtracted the reference-particle profile from the corresponding curves of 50S subunits containing one selected protonated protein by comparing the low-Q data points of the reference-particle scattering with those of the labeled-protein containing particles. The subtraction led to the intensity-difference curves which represent the intensities from the integrated protonated material.

The resulting intensity-difference curve together with those from other proteins are presented in the Guinier plots (Fig. 2). For small values of the momentum transfer Q ($Q = (4\pi/\lambda)\sin\theta$, with λ, the wavelength and 2θ, the full scattering angle), i.e. for small scattering angles, the Guinier approximation for the scattering intensity $I(Q)$ holds: $I(Q) \approx I(0)\exp(-\frac{1}{3}R_G^2Q^2)$ [25]. R_G is the radius of gyration, which can be derived from the slope of the regression line through the data points in a semilogarithmic plot (ln $I(Q)$ versus Q^2; Fig. 2, columns 1 and 3).

The Guinier approximation is only strictly valid for Q values very close to zero. For practical reasons, however, the innermost Q region is not accessible because of the need to eliminate the primary beam by using a beam-stop in front of the detector. In addition, the inner part of the scattering curve is often obscured by aggregation present in the sample preparations. The presence of aggregates can be distinguished from the rest of the scattering curve if their contribution decays very rapidly, and the added systematic error is then estimated to be small. Thus, in practice, it is only possible to use a restricted region for the determination of the radius of gyration; that region rarely exceeds $Q = 1/R_G$.

The arguments above hold for the isolated-protein curves. In the case of the in situ proteins, we observe some residual scattering even after subtraction of the reference-particle scattering, which, however, decays very rapidly compared to the protein contribution, so that one can only start the fitting procedure at larger but still acceptable Q values. Nevertheless, the fact that Q values up to $1.7/R_G$ are used may induce a small systematic error. This small error is tolerable, because (1) the straight line continues well beyond this value, and (2) as can be seen from Table 1 (column 3), the relative molecular masses of the proteins determined by extrapolation to $Q = 0$ are within a reasonable range around the sequence values with the exceptions of L1, L3 and L17 (see below). The R_G values derived are compiled in Table 1 (column 4).

All the operations for arriving at the protein scattering curves are linear, so that the error propagation calculations are straightforward. For mathematical (step-wise propagation due to the different procedures necessary to arrive at the difference curves) and statistical reasons (certain steps, like the scaling to the proton scattering are not independent), the propagated statistical error bars are, however, rather too large. Nevertheless, the statistical errors of the R_G determinations from r-proteins in situ were usually below $\pm 10\%$. The total maximal error was taken in most cases to be $\pm 10\%$ and reflects variations of the R_G values upon variation of the background subtraction and estimated preparative uncertainties. The latter argument was less significant in the cases of r-proteins in solution; in this case we maintain the statistical and estimated systematic (background subtraction) errors.

Assuming that to a first approximation the shapes of the proteins can be represented by ellipsoids of revolution, it is possible to calculate their half-axes by an iterative procedure from the R_G values and the masses of the proteins (R.P. May, unpublished). The corresponding prolate ellipsoid of revolution equivalents are displayed in Fig. 2 beside the Guinier plots (columns 2 and 4). The absolute dimensions of the ellipsoid equivalents are given in Table 1 (columns 7 and 8). Further, the relative molecular mass of the labelled component was determined from the forward scatter $I(0)$, which is derived from the intercept of the regression line with the y axis of the Guinier plot according to Ref. [26].

For the calculation of relative molecular masses M, we used a modified form of Jacrot and Zaccai's expression [26], which can be written as

$$M = \frac{I^{coh}(0)}{I_W c D_s T_s} \frac{(1 - T_W)\, g}{4\pi N_A} \left(\frac{M}{\sum b_i - \rho_b V} \right)^2 . \qquad (1)$$

$I^{coh}(0)$ is the coherent scattering of the sample at zero angle, I_W that of H_2O, c is the solute concentration in g/ml, D_s is the sample cell thickness, T_s and T_W are the sample and H_2O transmissions,

Table 1
Shape parameters for ribosomal proteins integrated into the 50S subunit (in situ) and isolated in solution (in sol.) as derived from small-angle neutron scattering (SANS)

Sample	M_r (seq)	M_r (SANS)	R_G (Å) ± error	Axial ratio (a/b)	$\mathscr{R}$ [b]	a (Å)	b (Å)
50S(L1)	24599	20400	20.3 ± 2.0	3.1	0.66	41.4	13.2
H-L1	24599	38100	25.4 ± 0.6	4.7		54.4	11.5
50S(L3) [a]	22258	26500	27.2 ± 2.7	5.6	1.22	59.0	10.5
H-L3	22258	40000	24.3 ± 0.5	4.6		52.0	11.2
50S(L4)	22087	17400	25.9 ± 2.6	5.2	0.95	55.9	10.8
H-L4	22087	19500	26.9 ± 4.0	5.5		58.3	10.5
50S(L6)	18832	18800	20.5 ± 2.1	3.8		43.0	11.3
50S(L7/12)	48880	43400	38.7 ± 3.9	6.5		84.6	13.0
50S(L10) [a]	17581	15100	22.6 ± 2.9	4.7		48.4	10.4
50S(L13) [a]	16019	20000	21.8 ± 2.2	4.7	1.47	46.6	10.0
H-L13	16019	19100	17.8 ± 0.3	3.2		36.4	11.4
H-L17	14365		17.6 ± 0.4	3.4		36.3	10.8
50S(L18)	12770	16400	19.7 ± 2.0	4.4	1.38	42.0	9.5
H-L18	12770	18200	16.4 ± 0.9	3.2		33.5	10.6
50S(L19)	13002	13600	24.1 ± 2.4	6.2		52.5	8.5
H-L22	12227	15200	19.0 ± 2.0	4.3		40.4	9.4
50S(L23)	11209	10100	14.6 ± 1.5	2.8	0.76	29.0	10.6
H-L23	11209	10600	16.9 ± 1.3	3.7		35.3	9.6
50S(L24)	11185	10400	16.7 ± 1.7	3.6	0.87	34.7	9.7
H-L24	11185	11600	18.0 ± 1.5	4.1		38.1	9.3

[a] One protein was removed from the deuterated TP50 for the preparation of the particle (see Material and Methods); in these cases a relative occupation number (protonated protein incorporated per deuterated subunit) of 1.0 was assumed for the determination of the relative molecular masses from the forward small angle scatter (M_r (SANS)), [24]); in all other cases the relative occupation number was assumed to be 0.9, according to the stoichiometry of protonated proteins used in the particle preparations. Assuming smaller values for the occupation numbers, some molecular masses improve significantly. The axial ratios a/b were calculated with the sequence molecular masses. H-L3 would have an axial ratio of 3.0 assuming that it is a dimer of 44516 daltons.

[b] The proportion of the two axial ratios is defined here as $(a/b)_{\text{in sol.}}/(a/b)_{\text{in sol.}}=\mathscr{R}$; $\mathscr{R}$ values deviating from 1 by up to 0.15, between 0.15 and 0.25, or more than 0.25 were defined as indication for weak, medium or strong conformational change during the assembly of the ribosome, respectively. A more precise distinction is not justified, since $\mathscr{R}$ is very sensitive with respect to R_G.

respectively. N_A is Avogadro's number. $\sum b_i$ is the sum of all scattering lengths within the volume V of a particle (protein), ρ_b the scattering length density of the buffer solution. Values of $\sum b_i/M$ are tabulated in [26]. Finally, g is a wavelength-dependent factor of a value close to 1 which accounts for inelastic and geometrical effects as well as for detector properties. With [26]

$$V = \frac{M}{N_A}\bar{v}, \tag{2}$$

one gets (May, unpublished)

$$M = \frac{I^{\text{coh}}(0)}{I_w c D_s T_s}\,\frac{(1-T_w)\,g}{4\pi}\,\frac{N_A}{(\Delta\rho\bar{v})^2}, \tag{3}$$

where $\bar{v}$ is the partial specific volume. This notation avoids the problem of knowing the real volume of a protein. For an average ribosomal protein, we assume $\Delta\rho\bar{v}$ to vary as

$$\Delta\rho\bar{v}(x) = (1.68 - 4.216x) \times 10^{10} \quad cm/g, \tag{4}$$

where x is the D_2O fraction in the buffer solution.

If only one component of a complex is visible for neutrons, the molecular mass M of the single component (M_c is the molecular mass of the complex) becomes (May, unpublished)

$$M = \left(\frac{I^{\text{coh}}(0)}{I_w c D_s T_s}\,\frac{(1-T_w)\,g}{4\pi}\,\frac{M_c N_A}{(\Delta\rho\bar{v})^2} \right)^{1/2}. \tag{5}$$

Coincidence of the relative molecular masses calculated from $I(0)$ with the corresponding values derived from protein sequencing is a valuable internal control for the validity of the scattering data. The

relative molecular masses calculated are given in Table 1 (column 3).

Relative molecular masses determined from $I(0)$ coincide quite well with the values derived from sequencing. Isolated L1 is an exception, where the $I(0)$-derived relative molecular mass deviates by about 50%. L3 seems to be a dimer in solution, and in the case of L17, the concentration measurement obviously was not consistent with the scattering data. Nevertheless, we included these measurements in Table 1 and Fig. 2, because the scattering data were of reasonable quality. The data were processed at least two times independently yielding consistent results. Data sets not yielding equivalent results in repeated processings were omitted or, alternatively, the corresponding particle was prepared and analysed again. This explains why some of the data presented deviates from that published previously [18].

The radii of gyration could be determined with an error of $\leqslant 10\%$ for most of the r-proteins listed. The respective prolate ellipsoids of revolution had an axial ratio of equal or greater than 2.8 in all cases.

4. Discussion

In this contribution we describe an attempt to gain insight into structural parameters of ribosomal proteins within the ribosomal matrix. Even though small-angle neutron scattering is the method best suited for this kind of measurement there are several obstacles to be overcome.

Only the small Q range can be used for obtaining shape information about ribosomal proteins in situ and in solution, for different reasons: The intensities fall off rapidly at larger Q values and thus render it problematic to extract reliable shape data. We suffered an additional loss in scattering intensity because the measurements had to be performed with small sample concentrations. The overall ribosome concentration was kept small enough to avoid interparticle interferences for the in situ measurements, but could not be too small since the mass fraction of one protein is only $\frac{1}{100}$ of that of a 50S subunit. Isolated ribosomal proteins, on the other hand, are only soluble in the mg/ml range.

The radius of gyration is the most direct shape parameter of a ribosomal protein that can be extracted from neutron-scattering measurements at small Q. With knowledge of the relative molecular mass of the respective protein the abstract number given by a radius of gyration can be translated into parameters describing a body, e.g. a prolate ellipsoid of revolution (Table 1), which approximates the overall extension of the ribosomal protein. Though an oblate ellipsoid of revolution satisfies the radius of gyration condition mathematically as well, the resulting very thin bodies are not a reasonable model for a protein's shape, in contrast to the prolate ellipsoids of revolution used here. All derived prolate ellipsoids had an axial ratio exceeding 2.8. This suggests a significant deviation from a spherical shape for all proteins measured within the ribosomal matrix as well as isolated in solution.

R_G values were determined for seven r-proteins within the ribosome as well as isolated in solution. Since the molecular weights derived from neutron scattering of three isolated proteins, L1, L3 and L18 deviated significantly from the corresponding values from the amino-acid sequences, we compare only the remaining four pairs in the following. Two out of these four R_G pairs differ significantly from each other (L13 and L23; Table 1, column 6), indicating a strong conformational change during the assembly process; two proteins, L4 and L24, appeared practically unchanged. A conformational change is not unexpected, since r-proteins probably have many hydrophobic contacts with their neighbours inside the ribosome. Isolated in aqueous solution these areas are forced into the interior of the protein molecule to minimize the water contact; assuming that this structure is somehow under tension, free energy will be released upon relaxation during its incorporation into the ribosome thus contributing to the assembly process.

Taking the relative change of the axial ratio of an ellipsoid as a measure for the strength of a conformational change of the respective r-protein, we distinguish weak ($\leqslant 15\%$), medium (15%–25%) and strong ($\geqslant 25\%$) conformational changes. In these terms protein L13 strongly changes its overall shape. This effect is less pronounced for protein L23. On the other hand, the shape variations for proteins L4 and L24 are well within the error that we estimated for small-angle neutron scattering and thus we clas-

sify these proteins as essentially retaining their solution shape within the ribosome. A more extended analysis should reveal whether or not the observed conformational changes are a common feature of the ribosomal assembly process.

Acknowledgement

We thank Dr. R. Brimacombe for help and advice.

References

[1] H.G. Wittmann, Ann. Rev. Biochem. 51 (1982) 155.
[2] F. Franceschi, S. Weinstein, U. Evers, E. Arndt, W. Jahn, H.A.S. Hansen, K. von Böhlen, Z. Berkovitch-Yellin, M. Eisenstein, I. Agmon, J. Thygesen, N. Volkmann, H. Bartels, F. Schlünzen, A. Zaytzev-Bashan, R. Sharon, I. Levin, A. Dribin, I. Sagi, T. Choli-Papadopoulou, P. Tsiboli, G. Kryger, W.S. Bennett and A. Yonath, in: The translational apparatus: structure, function, regulation, evolution, eds. K.H. Nierhaus, F. Franceschi, A. Subramanian, V.A. Erdmann and B. Wittmann-Liebold (Plenum Press, New York, 1993), p. 397.
[3] J. Frank, A. Verschoor, M. Rademacher and T. Wagenknecht, in: The Ribosome: structure, function, and evolution, eds. W.E. Hill, A. Dahlberg, R.A. Garrett, P.B. Moore, D. Schlessinger and J.R. Warner (American Society for Microbiology, Washington, 1990) p. 107.
[4] W.E. Hill, J.D. Thompson and J.W. Anderegg, J. Mol. Biol. 44 (1969) 263.
[5] A. Tardieu and P. Vachette, EMBO J. 1 (1982) 35.
[6] H.B. Stuhrmann, M.H.J. Koch, R. Parfait, J. Haas, K. Ibel and R.R. Crichton, Proc. Natl. Acad. Sci. USA 74 (1977) 2316.
[7] M. Oakes, E. Henderson, A. Scheinman, M. Clark and J.A. Lake, in: Springer Series in Molecular Biology. Structure, function, and genetics of ribosomes, eds. B. Hardesty and G. Kramer (Springer, Berlin, 1986) p. 47.
[8] M. Stöffler-Meilicke and G. Stöffler, in: The ribosome: structure, function, and evolution, eds. W.E. Hill, A. Dahlberg, R.A. Garrett, P.B. Moore, D. Schlessinger and J.R. Warner (American Society for Microbiology, Washington, 1990) p. 123.
[9] J. Walleczek, D. Schüler, M. Stöffler-Meilicke, R. Brimacombe and G. Stöffler, EMBO J. 7 (1988) 3571.
[10] R.P. May, V. Nowotny, P. Nowotny, H. Voss and K.H. Nierhaus, EMBO J. 11 (1992) 373.
[11] M.S. Capel, D.M. Engelman, B.R. Freeborn, M. Kjeldgaard, J.A. Langer, V. Ramakrishnan, D.G. Schindler, D.K. Schneider, B.P. Schoenborn, I.-Y. Sillers, S. Yabuki and P.B. Moore, Science 238 (1987) 1403.
[12] K.S. Wilson, K. Appelt, J. Badger, I. Tanaka and S.W. White, Proc. Natl. Acad. Sci. USA 83 (1986) 7251.
[13] V. Ramakrishnan and S.W. White, Nature 358 (1992) 768.
[14] M. Leijonmarck and A. Liljas, J. Mol. Biol. 195 (1987) 555.
[15] H.G. Wittmann, J.A. Littlechild and B. Wittmann-Liebold, in: Ribosomes: structure, function and genetics, eds. G. Chambliss, G.R. Craven, J. Davies, K. Davis, L. Kahan and M. Nomura (University Park Press, Baltimore, 1980) p. 51.
[16] D.H. Harrison, R.P. May and P.B. Moore, J. Appl. Cryst. 26 (1993) 198.
[17] M.Yu. Pavlov and I.N. Serdyuk, J. Appl. Cryst. 20 (1987) 105.
[18] V. Nowotny, R.P. May and K.H. Nierhaus, in: Springer Series in Molecular Biology. Structure, function, and genetics of ribosomes, eds. B. Hardesty and G. Kramer (Springer, Berlin, 1986) p. 101.
[19] K.H. Nierhaus and F. Dohme, Methods Enzymol. 59 (1979) 443.
[20] R.M. Kamp, A. Bosserhof, D. Kamp and B. Wittmann-Liebold, J. Chrom. 317 (1984) 181.
[21] P. Nowotny, H. Eckardt, V. Nowotny and R.M. Kamp, Chromatographia 25 (1988) 409.
[22] P. Nowotny, V. Nowotny, H. Voss and K.H. Nierhaus, Methods Enzymol. 164 (1988) 131.
[23] P. Lindner, R.P. May and P.A. Timmins, Physica B 180/181 (1992) 967.
[24] K. Ibel and H.B. Stuhrmann, J. Mol. Biol. 92 (1975) 255.
[25] A. Guinier and G. Fournet, Small angle scattering of X-rays (Wiley, New York, 1955).
[26] B. Jacrot and G. Zaccai, Biopolymers 20 (1981) 2413.